Spinodal decomposition during bulk copolymerization: reaction injection moulding

Anthony J. Ryan*
Department of Chemical Engineering and Materials Science, University of Minnesota, Minneapolis, MN 55455, USA
(Received 14 March 1989; accepted 7 June 1989)

Phase separation in segmented copolyureas and copoly(urethane–urea)s formed by reaction injection moulding (RIM) has been investigated by studies of the formation of model polyurea–polyether blends with no covalent bonds between the phases. The polyblends have similar thermal and small-strain mechanical properties to the analogous copolymers. Removal of 80% of the polyether by selective solvent extraction indicates the continuity of the polyether phase. Electron micrographs of the isolated polyurea show a random–continuous polyurea structure with a wavelength of ≈ 200 nm. The experimental data are interpreted in terms of the polymerization being equivalent to a thermodynamic quench from one-phase space into two-phase space. Thus the co-continuity of the phases is characteristic of the early stages of spinodal decomposition and has been retained by vitrification of the polyurea.

(Keywords: spinodal decomposition; phase separation; reaction injection moulding; polyureas)

INTRODUCTION

Reaction injection moulding (RIM) is a method for the high speed production of complex polymer parts directly from low viscosity monomers or oligomers. The reactants are combined by high pressure impingement mixing and then they fill a mould, under low pressure, where they complete the reaction to give a polymer. The formation of solid polymeric materials involves crosslinking or (micro)phase separation, or a combination of the two phenomena, and parts can often be demoulded in less than one minute. A good review of the fundamental science which underpins RIM has recently been published by Macosko[1].

RIM materials are generally segmented block copolymers and previous studies of phase separation in RIM have led to the hypothesis[2] that for the fastest systems, such as highly catalysed polyurethanes[3], poly(urethane–urea)s[4] and polyureas[5,6], which gel in <2 s, the dominant phase separation process is spinodal decomposition.

Scheme 1 shows the chemistry of formation of an $(AB)_n$ block copolyurea by bulk copolymerization. Only in the limit of complete reaction is such a copolymer formed and in the early stages of reaction the polymerizing mixture contains unreacted monomer, homopolymer, AB diblock copolymers, ABA triblock copolymers and higher homologues. It is well established that phase separation competes with polymerization, even in the very early stages of these types of reaction. The work of Yang and Macosko[7] has shown that hydrogen bonded structures appear in polyurethane forming systems when the average hard segment sequence length is only ≈ 1.8. Thus, the interpretation of phase separation in RIM falls into the universality class of a polymer mixture and not that of a block copolymer.

Theoretical[8,9] and experimental[10,11] studies of monodisperse diblock copolymers have shown that a fluctuation induced, first-order, order–disorder transition occurs to form a periodic free energy minimizing structure at the microphase–separation transition (MST) in these systems. Such a symmetrical situation is not envisaged in the dynamic competition between polymerization and phase separation found in RIM bulk copolymerizations.

A generalized phase diagram for a polymer mixture is shown in *Figure 1*. Conventionally the abscissa is labelled composition and the ordinate temperature. More recently the term $1/\chi N$, where χ is the Flory–Huggins[12,13] interaction parameter and N is the polymerization index, has been shown to be parametrically equivalent to the temperature. Thus bulk copolymerization, which changes χ and increases N, is parametrically equivalent to quenching a polymer mixture. Three types of quenching or polymerization experiments are shown in *Figure 1*:

(1) from a position in one-phase space to another in one-phase space;
(2) from a position in one-phase space to a position in the metastable region;
(3) from a position in one-phase space to a position below the spinodal curve.

In experiment (1) no phase separation occurs. In experiment (2) phase separation may occur by nucleation and growth and in experiment (3) phase separation will occur by spinodal decomposition. (A mono-disperse block copolymer, because it has a different universality class from a polymer blend or a mixture of block copolymer, homopolymers and monomer, would undergo a first order, order–disorder transition in experiment (3) to give a microphase separated, periodic, free energy minimizing structure.)

The nucleation and growth process is shown schematically in *Figure 2*[14]. This process occurs when a mixture is in the metastable region and is stable to

* Current address: Manchester Materials Science Centre, UMIST, Grosvenor Street, Manchester M1 7HS, UK

0032-3861/90/040707-06

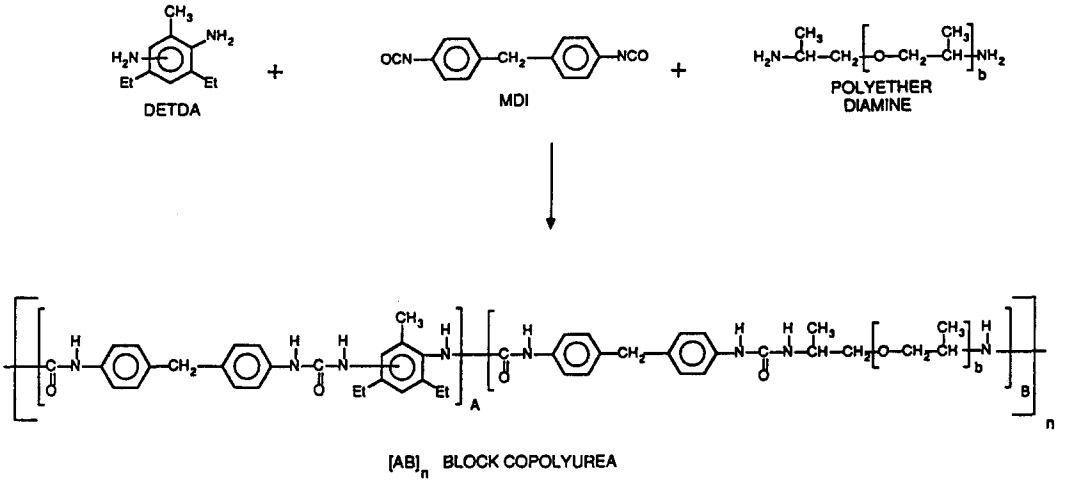

Scheme 1

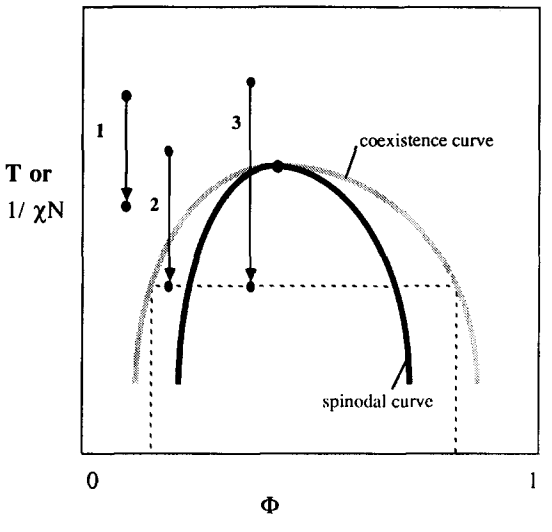

Figure 1 Schematic phase diagram of a polymer mixture

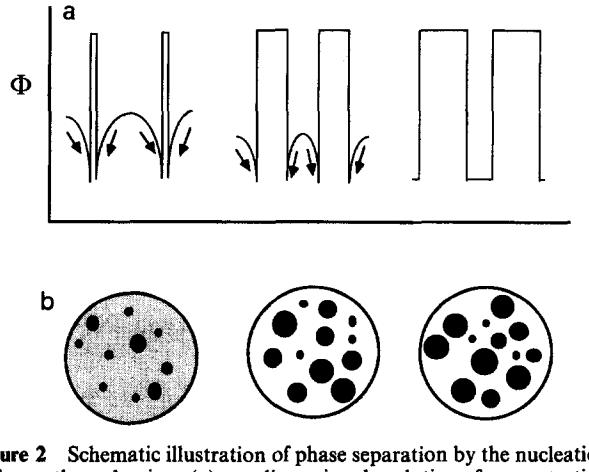

Figure 2 Schematic illustration of phase separation by the nucleation and growth mechanism: (a) one-dimensional evolution of concentration profiles; (b) two-dimensional representation of the resultant phase structure

infinitesimal (thermal) concentration fluctuations but is unstable at sufficiently large concentration fluctuations where nuclei are formed. Once the energy barrier has been overcome by the formation of nuclei, randomly in space and time, these nuclei then grow. The molecules or chain segments that feed the new phase follow the

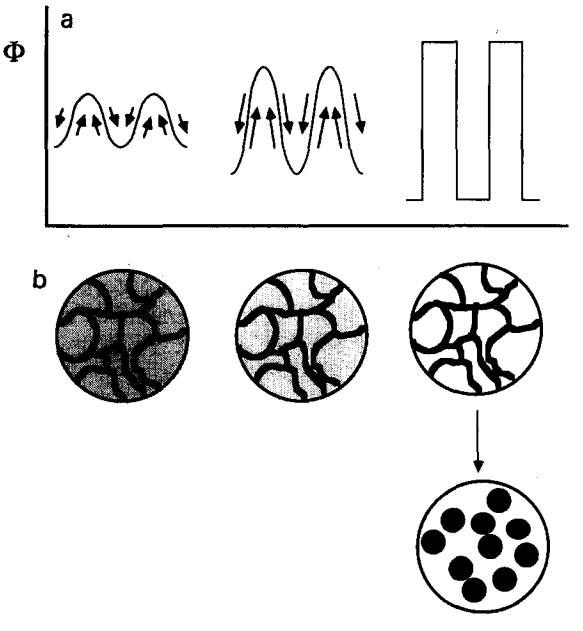

Figure 3 Schematic illustration of phase separation by spinodal decomposition: (a) one-dimensional evolution of concentration profiles; (b) two-dimensional representation of the resultant phase structure

ordinary transport phenomena with a positive diffusion coefficient ('downhill' diffusion). The early stages of the phase separation process are characterized by the existence of a continuous-phase, dispersed-phase morphology. (Only if the nuclei grow to such an extent that they reach the percolation limit and coalesce will they achieve continuity of the area-minimizing morphologies of rods or lamella.)

The spinodal decomposition process is shown schematically in *Figure 3*[14]. In the unstable region of the phase diagram (beneath the spinodal curve) the mixture is unstable to infinitesimal concentration fluctuations, there is no thermodynamic barrier to phase growth and thus phase separation occurs by a continuous and spontaneous process. Since the mixture is initially uniform in composition, this spontaneous process must occur by a diffusional flux against the concentration gradient. Thus the process occurs by 'uphill' diffusion with a negative diffusion coefficient. The process is characterized by a bicontinuity of phases in the early

stages of the process though this feature may be lost through Ostwald ripening as the system seeks to minimize its free energy by minimizing its interfacial area.

We have recently reported[2] that the moduli of a wide range of RIM copolymers, both poly(urethane–urea)s and polyureas, give a good fit to the Davies[15] equation for the modulus of materials with co-continuous phases. Furthermore, dynamic mechanical analysis and comparisons of the predicted and measured degrees of (micro)phase separation, indicate that these materials do not have equilibrium morphologies. Thus it was hypothesized[2] that the co-continuity of the phases was characteristic of the spinodal decomposition process and that this structure was frozen in as the hard segments vitrify during phase separation.

Even the determination of the morphology of well characterized polyurethanes with equilibrium morphologies is fraught with difficulties[16,17]. Both Chen-Tsai[18] and Li[17] have investigated the morphology of specially synthesized, stainable, polybutadiene-containing polyurethanes and there are still some unsolved areas in the composition–morphology spectrum. We have attempted to image, by transmission electron microscopy, the morphology of RIM poly(urethane–urea)s but could only show diffuse structures on the >30 nm scale[5]. Willkomm and co-workers[6] have reported small angle X-ray scattering (SAXS) studies of polyurea RIM materials. Structures of the order of >10 nm (which is approximately the radius of gyration of the soft segment oligomer) were observed and the materials were reported to have sharp microphase boundaries and no long range order. Analysis of the kinetics of phase separation for these fast polymerizing systems has proved to be beyond the ability of current experimental techniques.

To investigate further the phase separation processes occurring during RIM, we present studies of a model system with the hard segment polymerization occurring in a solvent of unreactive polyether (a polyether diamine which has been capped with phenyl isocyanate). This model system will yield a blend of polyether and polyurea with no covalent bonds between the phases. Thus isolation of the hard segment phase, by selective extraction of the low molecular weight polyether, will allow us to study the morphology with greater confidence.

EXPERIMENTAL

Reactants

The polyisocyanate, LF168 (ICI Americas), was a low viscosity, uretonimine modified version of 4,4′-methylene-bis-phenyl isocyanate, MDI, with an average functionality of 2.15 and an equivalent weight of 143 g mol^{-1} isocyanate groups. The chain extender, DETDA (Ethyl Corporation), a mixture of 3,5-diethyl toluene-2,4-diamine and 3,5-diethyl toluene-2,6-diamine, comprised 77% of the 2,4-diamine, 18% of the 2,6-diamine and 5% of other amines. The unreactive soft segment was formed from a stoichiometric mixture of phenyl isocyanate (Aldrich) and Jeffamine D2000 (Texaco Chemical Company), a 2000 molecular weight polyoxypropylene diamine. All materials were used as received.

Reaction injection moulding

A mini-RIM machine with lever arm control was used in this study. The machine and its operation are described in detail elsewhere[19]. Machine volume ratio was calibrated using liquid petroleum and shown to be $\pm 0.5\%$. To maintain functional group stoichiometry of 1.0 the volume ratios were set at 2.49 and 4.67 for the 50% and 30% polyurea materials respectively. The mixhead was based on the design of Macosko and McIntyre[20] and this type of mixhead allows reactant recycle before impingement mixing. Polyamine Reynolds numbers were ≈ 800 to ensure good mixing; adiabatic temperature rise data[21] shows no Reynolds number dependence in the range 500–1000 for the corresponding system containing free D2000. After mixing the reactive mixture passes through a dam–gate aftermixer assembly and into a rectangular mould of dimensions $280 \times 100 \times 3$ mm.

DETDA and capped D2000 were blended, degassed and loaded into one side of the RIM machine and LF168 was loaded into the other side. The tanks were then blanketed with nitrogen and the materials heated up to 90 and 60°C, respectively. The mould temperature was 110°C and plaques were removed from the mould after 2 min.

Polymer characterization

A differential scanning calorimeter (TA 3000, Mettler Inc.) was used for heat capacity measurements to examine the polyether glass transition temperature, T_g^S. The heating rate was 5°C min^{-1} and dry nitrogen was used as a purge gas with a sample mass of 10–20 mg. Dynamic mechanical analysis (DMA; System IV, Rheometrics Inc.) was performed in the torsion rectangular mode at 1 Hz. Test bars with dimensions $30 \times 10 \times 3$ mm were cut from RIM plaques. Measurements were shown to be strain insensitive in the region used and were made in a nitrogen atmosphere at a heating rate of 2°C min^{-1} from -100 to 300°C.

Preferential extraction of the unreactive polyether was accomplished by continuous Soxhlet extraction, with n-propanol, to constant weight. At least 80% by weight of the polyether was extracted in this manner. To prepare samples for scanning electron microscopy, internal fracture surfaces of extracted and as-moulded materials were given a thin carbon coating. A scanning electron microscope (SEM 840, JEOL Inc.) was used at an accelerating voltage of 5 kV and a working distance of ≈ 10 mm to obtain the micrographs.

RESULTS AND DISCUSSION

The use of an aromatic urea-terminated polyoxypropylene oligomer as a solvent for the DETDA/MDI reaction leads to a similar driving force to phase separation for the blend and the copolymer, at least in the limit of low conversion. The physical gel time (vitrification time) of the 50% polyurea–polyether blend was ≈ 1.0 s and this corresponds to ≈ 1.3 s for the analogous 50% hard segment copolyurea reported by Willkomm[6]. Copolyureas are normally translucent, due to the size scale of (micro)phase separation, and, at the mould temperatures used in this study, tough. The model polyblends obtained were opaque and either dry and brittle (50% polyurea) or

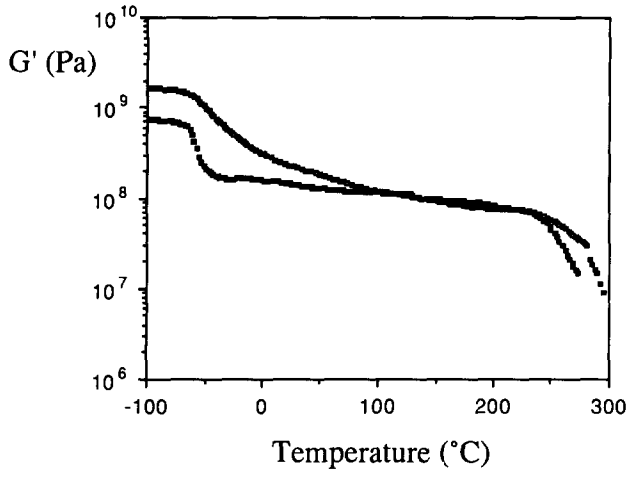

Figure 4 Shear storage modulus, G', *versus* temperature for the as-moulded 50% polyurea–polyether blend (■) and the corresponding RIM copolyurea (□)[5]

sticky and soft (30% polyurea) but both could be removed from the mould in one piece.

Differential scanning calorimetry (d.s.c.) studies showed that the polymers are well phase separated. Both the 50% and 30% polyurea materials have a T_g^S of $-58°C$, which is identical to that of the phenyl isocyanate capped D2000 and in contrast to the value of $-50°C$ reported for the analogous copolyureas[6] which are more phase-mixed. The extracted materials show no detectable thermal transitions in the temperature interval -100 to 100°C and any polyoxypropylene oligomer remaining in these samples must be dissolved in the polyurea phase. (Such dissolution could be aided by hydrogen bonding of the urea end groups and possibly even formation of some block copolymer by transureafication reactions. To avoid such ambiguities synthesis of alkyl-ether capped polyethers is currently being pursued.)

Shear storage modulus, G', and mechanical damping, tan δ, *versus* temperature curves are presented in *Figures 4* and *5*, respectively, for the as-moulded 50% polyurea blend and the corresponding RIM material. Both the copolyurea and the polyblend still possessed some structural integrity after being removed from the mechanical spectrometer furnace at 260°C.

Because of the common feature of chemical structure and a phase separated morphology there are a number of qualitative similarities between the DMA curves of the polyblend and the analogous copolyurea. There is a half decade drop in G' and a corresponding peak in tan δ associated with the glass transition of the polyoxypropylene oligomer at $\approx -50°C$. This is followed by a long modulus plateau over a range of $\approx 250°C$ and above 200°C there is a peak in tan δ and a catastrophic drop in modulus associated with the polyurea glass transition T_g^H.

The differences in detail between the two sets of DMA curves is due to the differences in the size scale and degree of phase separation caused by the absence of interphase covalent bonds in the polyblend. The absolute value of the polyblend G' is lower than that of the copolyurea below T_g^S, due to the differences in coefficients of thermal expansion between polyurea and polyether and the lack of any interfacial covalent bonds. The peak in tan δ associated with T_g^S is broader and shifted to higher temperatures for the copolyurea material and this is a function of its reduced degree of phase separation and its diffuse phase boundaries. Furthermore, the greater value of copolyurea G' between T_g^S and 100°C, the greater sensitivity of modulus to temperature and the higher mechanical damping of the copolyurea than of the polyblend are also due to the existence of phase mixed material in the copolyurea. T_g^H is seen as a peak in tan δ and a corresponding drop in modulus for the polyblend, whereas the behaviour of the block copolymer is more complex*. There is a broad peak in tan δ associated with local motion in the polyurea-rich phase followed by an increase in tan δ and a catastrophic drop in modulus as the copolyurea begins to degrade at $\approx 300°C$. The most obvious feature of the DMA curves is the relative insensitivity of modulus to temperature in the temperature interval 50–200°C. Previous studies of copolyureas[6] refer to this as a 'rubbery plateau' and this has a value of ≈ 100 MPa for both the copolyurea and the polyblend. The 'rubbery plateau' invoked is the modulus of a system of rubbery chains crosslinked through isolated, hydrogen bonded, glassy, polyurea domains. For the polyblend there are no covalent bonds between the polyether and polyurea and the modulus is due entirely to the existence of a continuous polyurea phase. The value of G' for the copolyurea suggests that it too has a continuous polyurea phase and more recent studies of RIM copolyureas and copoly(urethane–urea)s have shown them to have moduli very close to those predicted for materials with co-continuous morphologies[3].

Figures 6 and *7* are scanning electron micrographs of the internal fracture surfaces of n-propanol-extracted 50% and 30% polyurea–polyether blends, respectively. The detail in the self-supporting, continuous, polyurea materials is quite spectacular. The 'empty' phase can be seen extending back into the sample and the extraction of 80% of the polyether, from samples that had dimensions $10 \times 10 \times 3$ mm, indicates that there was a continuous pathway through the polyether phase. Although the structure is random and co-continuous there appears to be a constant length scale of ≈ 200 nm for the 50% polyurea blend. A random–co-continuous structure with a constant wavelength is typical of the

* The existence of a glass transition for the MDI/DETDA system is still in dispute. Most authors[3–5] observe peaks in tan δ at elevated temperatures, but there is always evidence of some degradation coincident with the onset of segmental motion

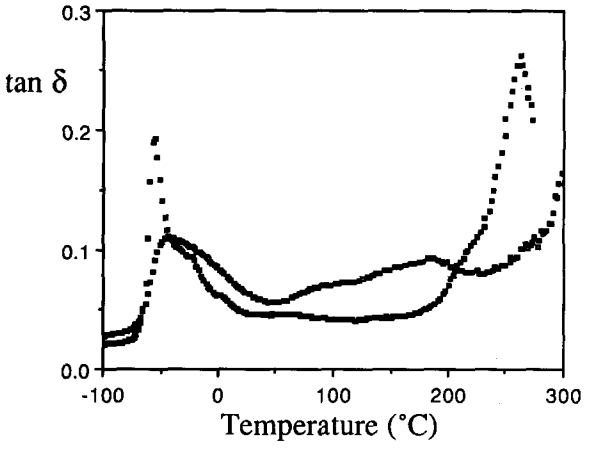

Figure 5 Mechanical damping, tan δ, *versus* temperature for the as-moulded 50% polyurea–polyether blend (■) and the corresponding RIM copolyurea (□)[5]

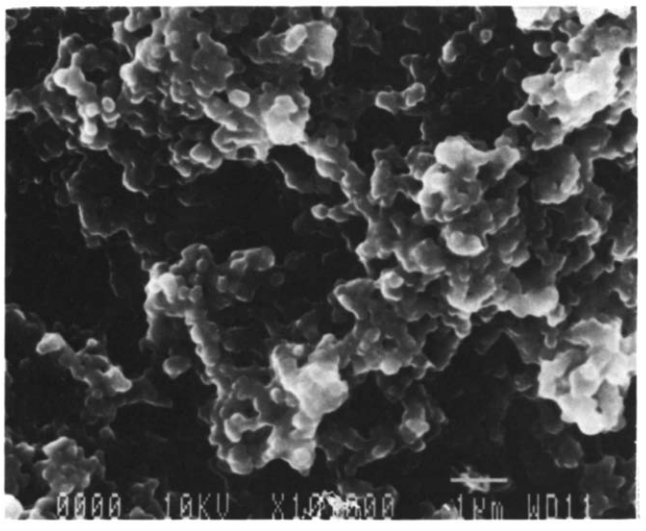

Figure 6 Scanning electron micrograph of the internal fracture surface of the n-pronanol extracted 50% polyurea–polyether blend

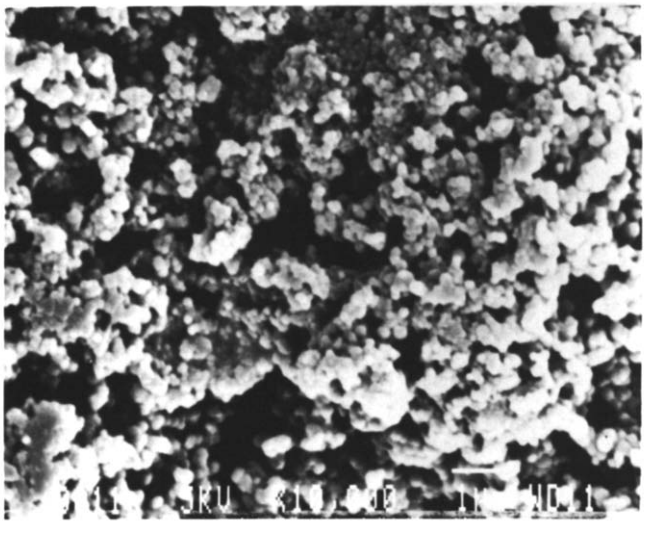

Figure 7 Scanning electron micrograph of the internal fracture surface of the n-propanol extracted 30% polyurea–polyether blend

early stages of spinodal decomposition[14]. Some 'ripening' has taken place in both cases and the more spheroid appearance of the 30% polyurea network could be due to the system having progressed to the situation where free energy is minimized by the minimization of the interfacial area, but the structure is not that formed by the coalescence of spheres (the percolation limit for an arrangement of spheres being $\approx 67\%$). An alternative explanation of the more spheroid appearance of the continuous 30% polyurea could be that it passed through the metastable region of the phase diagram during the composition quench and some nucleation and growth occurred before spinodal decomposition.

There have been a number of other micrographs of structures formed by liquid–liquid phase separation (spinodal decomposition). Hikmet *et al.*[22] investigated phase separation in the atactic-polystyrene/cyclohexanol system and were able to image isolated polystyrene foam structures at low volume fractions of polymer, depending on the quenching conditions used, the evolving structure could be captured at various stages of 'ripening'. Aubert[23] has investigated the isotactic-polystyrene/nitrobenzene system and has also been able to image isolated foam structures with regular, $>1\,\mu m$, cell structures. Sperling[24] has studied the phase separation and morphology of interpenetrating polymer networks (IPN). In one specific case the linear portion of a semi-IPN was extracted and the morphology imaged by SEM. The micrograph of the extracted material is remarkably similar to those obtained in this study, but no mechanism of phase separation was reported for these materials.

Figure 8 is a micrograph of an internal surface of the as-moulded material. The high fracture surface area of this material is due to the interstices of the brittle polyurea network (or foam) being filled with a viscous polyoxypropylene liquid which has a low surface tension. In contrast, *Figure 9* is a micrograph of the internal fracture surface of a 50% hard segment copolyurea and apart from some tearing marks around a void (a feature was required for focusing purposes) the surface is completely featureless at this magnification.

SUMMARY AND CONCLUSIONS

Phase separation and morphology development during copolyurea formation have been studied via a model

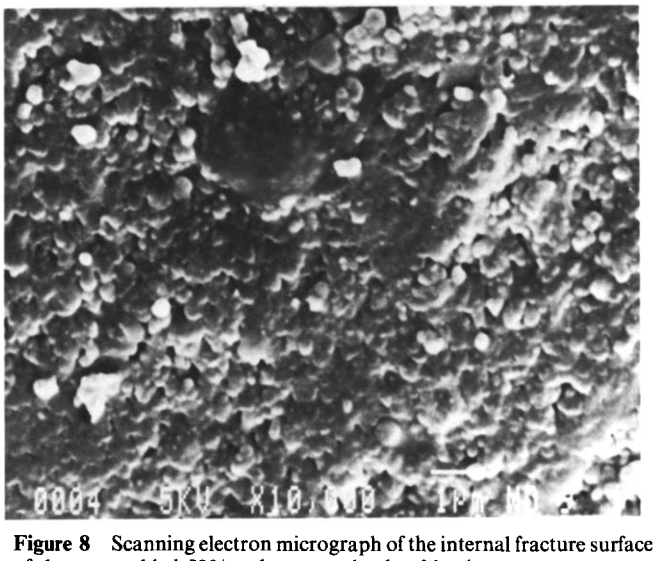

Figure 8 Scanning electron micrograph of the internal fracture surface of the as-moulded 50% polyurea–polyether blend

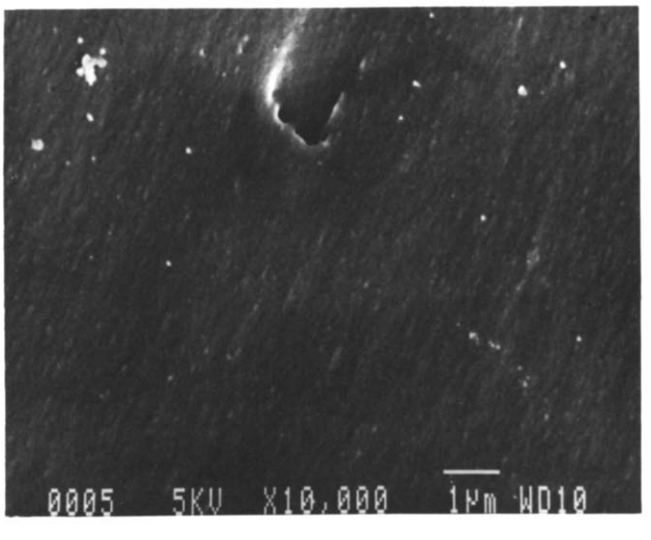

Figure 9 Scanning electron micrograph of the internal fracture surface of the as-moulded 50% hard segment RIM copolyurea

polymer blend. D.s.c. and DMA show the model materials to have thermal and small-strain mechanical properties similar to the analogous copolyureas. The preferential extraction of 80% of the polyether through samples of thick cross section indicates the existence of a continuous polyether phase. Examination of the resulting morphology shows the polyurea to be continuous and random with a size scale of ≈ 200 nm.

Thus it is concluded that the model system undergoes spinodal decomposition due to the polyurea-forming reaction acting as a large thermodynamic quench (an increase in χN) from the one phase region of the phase diagram into the unstable region of the phase diagram. The co-continuity of the phases is due to the arrest of the spinodal decomposition process by vitrification of the polyurea.

The model materials fail to recreate accurately the dynamics of the copolyurea-forming system on a number of counts. There are no covalent bonds between the phases and, as such, the viscosity of the mixture, the reaction kinetics and the interfacial energy of the system will be significantly different from the copolyurea, thus perturbing the phase separation process. This is manifest in the size scale of the phase separation being approximately twenty times larger than the microphase separation observed by SAXS for the copolyureas[6].

The extrapolation of this model study to the copolyurea and copoly(urethane–urea) systems is reasonable given the evidence of (micro)phase continuity in these materials[2]. However, further experiments, such as dynamic SAXS, are required to determine the (micro)-phase separation mechanism during RIM.

ACKNOWLEDGEMENTS

The author is grateful to Professor C. W. Macosko for the hospitality afforded during his stay in Minnesota. Stimulating discussions with Dr F. S. Bates, Professor C. W. Macosko, Dr J. L. Stanford, Dr R. H. Still, Mr W. R. Willkomm and Mr A. N. Wilkinson are acknowledged. Mr S. C. Scott and Mr W. R. Willkomm assisted with SEM and DMA, respectively. This work was funded by a NATO Research Fellowship.

REFERENCES

1 Macosko, C. W. 'RIM Fundamentals', Hanser, Munich, 1988
2 Ryan, A. J., Stanford, J. L. and Still, R. H. *Plast. Rubb. Proc. Appl.* in press
3 Camargo, R. E., Macosko, C. W., Tirrell, M. and Wellinghof, S. T. *Polym. Sci. Technol.* 1982, **18**, 95
4 Ryan, A. J., Stanford, J. L. and Still, R. H. *Br. Polym. J.* 1988, **20**, 77
5 Ryan, A. J., Stanford, J. L. and Wilkinson, A. N. *Polym. Bull.* 1987, **18**, 577
6 Willkomm, W. R., Chen, Z. S., Macosko, C. W., Gobran, D. A. and Thomas, E. L. *Polym. Engng. Sci.* 1988, **28**, 888
7 Yang, W. P. and Macosko, C. W. *J. Makromol. Symp.* 1989, **25**, 23
8 Leibler, L. *Macromolecules* 1980, **13**, 1602
9 Frederickson, G. H. and E. Helfand, *J. Chem. Phys.* 1987, **87**, 697
10 Bates, F. S. *Macromolecules* 1984, **17**, 2607
11 Bates, F. S. and Hartney, M. A. *Macromolecules* 1985, **18**, 2478
12 Flory, P. J. *J. Chem. Phys.* 1942, **10**, 51
13 Huggins, M. L. *J. Phys. Chem.* 1942, **46**, 151
14 Olabisi, D., Robeson, L. M. and Shaw, M. T. 'Polymer–Polymer Miscibility', Academic Press, New York, 1979
15 Davies, W. E. A. *J. Phys. D Appl. Phys.* 1971, **4**, 1176
16 Roche, E. J. and Thomas, E. L. *Polymer* 1981, **22**, 333
17 Li, C., Goodman, S. L., Albrecht, R. M. and Cooper, S. L. *Macromolecules* 1988, **21**, 2367
18 Chen-Tsai, C. H. Y., Thomas, E. L., MacKnight, W. J. and Schnieder, N. S. *Polymer* 1986, **27**, 659
19 Lee, L. J. and Macosko, C. W. *SPIE ANTEC Tech. Pap.* 1978, **24**, 151
20 Macosko, C. W. and McIntyre, D. B. US Patent 4,473,531, 1984
21 Pannone, M. C. and Macosko, C. W. *Polym. Engng. Sci.* 1988, **28**, 660
22 Hikmet, R. M., Callister, S. and Keller, A. *Polymer* 1988, **29**, 1378
23 Aubert, J. *Macromolecules* 1988, **21**, 3468
24 Widmaier, J. M. and Sperling, L. H. *Macromolecules* 1982, **15**, 625